

Oxygen-Vacancy Ordering in the $\text{YBa}_2\text{Cu}_3\text{O}_z$ Basal Plane Studied by the Cluster Variation Method

A. Berera,^{1,2} L. T. Wille,¹ and D. de Fontaine^{1,3}

Received November 16, 1987

The cluster variation method is used to calculate a phase diagram for a two-dimensional Ising model representing the Cu_2O plane of the high- T_c superconductor $\text{YBa}_2\text{Cu}_3\text{O}_z$. Both first (V_1) and second-neighbor (V_2) interactions are considered, with $V_2/V_1 = -\frac{1}{2}$. At high temperatures, the transition from the disordered (tetragonal) to the ordered (orthorhombic) phase is second-order. A tricritical point is found below which phase separation occurs. Fractional site occupancy and second-neighbor pair correlations are calculated as a function of temperature. The relevance of the model to the thermodynamics of ordering in the high- T_c compound is discussed.

KEY WORDS: Two-dimensional Ising model; cluster variation method; superconductors.

The tetragonal ($P4/mmm$) to orthorhombic ($Pmmm$) phase transition which occurs in the superconducting compound $\text{YBa}_2\text{Cu}_3\text{O}_z$ appears to be caused by a rearrangement of oxygen atoms on the available lattice sites in the Cu_2O basal plane.⁽¹⁾ This ordering process can thus be mapped onto a two-dimensional Ising model with a rather peculiar set of effective pair interactions between oxygen sites.^(2,3) We consider first-neighbor interactions (V_1) and second-neighbor interactions: V_2 denoting those mediated by the Cu atoms and V_3 denoting those that are not.

The interaction scheme proposed here is described in Fig. 1a, which shows the arrangement of oxygen (\circ) and vacant (\square) sites for the

¹ Materials and Chemical Sciences Division, Lawrence Berkeley Laboratory, Berkeley, California 94720.

² Department of Physics, University of California Berkeley, California 94720.

³ Department of Materials Science and Mineral Engineering, University of California, Berkeley, California 94720.

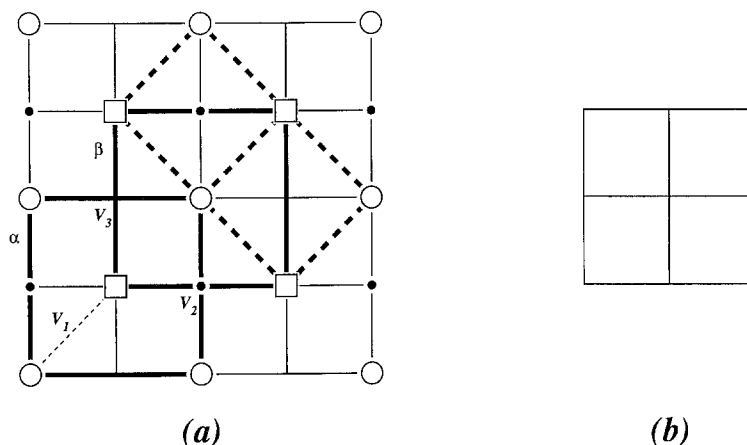


Fig. 1. The Cu_2O basal model. (a) (●) Cu atoms, (○) oxygen, and (□) vacant sites. (b) CVM motif. Translation of this motif on the structure shown in (a) gives rise to four types of clusters: α and β five-point centered squares (heavy outline) and two four-point squares (heavy dashed outlines), one centered on Cu atoms, the other not. Pair interactions V_1 , V_2 , V_3 are indicated.

perfectly ordered orthorhombic phase. Small, filled circles represent Cu atoms. In such an arrangement, one square sublattice (α) is completely occupied by ○ symbols, the other (β) by □ symbols. This arrangement produces long, parallel O–Cu–O chains, believed to be responsible for the superconducting properties of $\text{YBa}_2\text{Cu}_3\text{O}_z$.

It was shown elsewhere by ground-state analysis⁽³⁾ that, for the interaction set V_1 , V_2 , V_3 , other ordered arrangements in addition to that depicted in Fig. 1 are possible. In particular, a period doubling structure was predicted^(2,3) which was also discovered by high-resolution transmission electron microscopy and diffraction.⁽⁴⁾

Since the superconducting transition depends critically on the state of order in the CuO_2 basal plane,⁽¹⁾ it is essential to calculate phase diagrams for various choices of the ratios V_2/V_1 and V_3/V_1 . In this paper we examine only the case $V_2 = V_3 = -\frac{1}{2}V_1$, $V_1 > 0$, the convention adopted being that a positive interaction parameter favors unlike (antiferromagnetic) coupling. The case $V_2 \neq V_3$ is currently under study. The chosen values were selected because (a) they guaranteed the structure of Fig. 1 as a stable ground state at stoichiometry and (b) other statistical mechanical calculations, performed on the very same model, were available to check the validity of the computational method used here, namely the cluster variation method (CVM).⁽⁵⁾ Oxygen–vacancy long-range ordering has been studied recently by a quasichemical approximation,^(6,7) but only with nearest neighbor interactions and short-range correlations.

The basic motif for the CVM calculation was chosen to be the figure consisting of four small squares shown in Fig. 1b. Translation of this motif on the Cu_2O basal plane structure yields four types of clusters, two five-point (heavy outlines) and two four-point clusters (heavy dashed lines), one containing Cu, the other not. The same types of clusters were used previously in another context,^(8,9) demonstrating that the CVM in the four-point/five-point cluster approximation gave a critical temperature at zero field for the nearest neighbor Ising model only 4% higher than the exact Onsager solution. A simpler CVM approximation involving only the four-point cluster was recently proposed by Bell,⁽¹⁰⁾ but no phase diagram was reported. The choice of the five- and four-point cluster combination was suggested to us by R. Kikuchi;⁽¹²⁾ it was further justified by general theoretical arguments recently described in detail by Finel.⁽⁹⁾ The CVM entropy formula was derived by J. Kulik⁽¹¹⁾ and by R. Kikuchi⁽¹²⁾ and can be found in Finel's doctoral dissertation.⁽⁹⁾

The CVM-calculated phase diagram, symmetric about the oxygen concentration $c_{\text{O}} = \frac{1}{2}$, is shown in Fig. 2. At low concentrations and high temperatures the two-dimensional disordered phase $4mm$ of square symmetry is calculated to be the stable one. It corresponds to the three-dimensional tetragonal phase $P4/mmm$. A line of second-order transitions (heavy dashed line) separates the disordered phase region from that of the ordered phase mm (in our previous publication, the full international symbol $p2mm$ was used). This phase of rectangular symmetry corresponds to the three-dimensional orthorhombic phase $Pmmm$, which is the superconducting one. The upper ordering critical point at stoichiometry $c_{\text{O}} = 0.5$ lies at a reduced temperature $kT_0/V_1 = 4.03$, whereas high-temperature series expansions⁽¹³⁾ give the value $kT_0/V_1 = 3.80$.

The line of second-order transitions ends at a tricritical point (t), which has coordinates $kT_t/V_1 = 1.41$, $c_{\text{O}} = 0.19$, and $\mu = 3.94$, where the field variable μ represents a difference of chemical potentials $\mu_0 - \mu_{\square}$. These values are to be compared to those obtained from renormalization group techniques by Rikvold *et al.*⁽¹⁴⁾ $kT_t/V_1 = 1.205 \pm 0.003$, $c_{\text{O}} \approx 0.30$, and $\mu/V_1 = 3.965 \pm 0.001$, and by Claro and Kumar,⁽¹⁵⁾ $kT_t/V_1 = 1.28$ and $c_{\text{O}} \approx 0.31$, in reasonable agreement with Monte Carlo results.⁽¹⁶⁾ An "interface method" calculation by Slotte⁽¹⁷⁾ gives, for the tricritical temperature, $kT_t/V_1 \cong -2.27V_2$ at $\mu/V_1 = 4$. Finally, it was pointed out by Huse⁽¹⁸⁾ that the tricritical point can be obtained exactly as a special case of Baxter's solution of the hard-hexagon model. The tricritical temperature in units of V_2 is $kT_t = 0.55802$.

Detailed calculations of phase boundary lines in the immediate vicinity of the tricritical point indicate that properties derived by Allen and Cahn⁽¹⁹⁾ on the basis of the Landau theory are well obeyed here: the dis-

ordered phase boundary joins the line of second-order transitions with no change in slope, unlike the case for the ordered phase boundary at point t . The fine dashed line is the metastable extension of the line of second-order transitions and represents an ordering spinodal,⁽²⁰⁾ i.e., a line below which the disordered phase becomes marginally unstable to small-amplitude ordering fluctuations. The fine, dot-dash curve is the locus of marginal instability for phase separation on the partially filled oxygen sublattice. In terms of the stability analysis presented earlier,⁽²⁾ the fine, dashed curve is the stability limit for two $\langle OO \rangle$ ordering waves operating, in phase opposition, on the two square sublattices of oxygen sites, and the dot-dash curve is the stability limit for a single $\langle OO \rangle$ wave acting on the partially

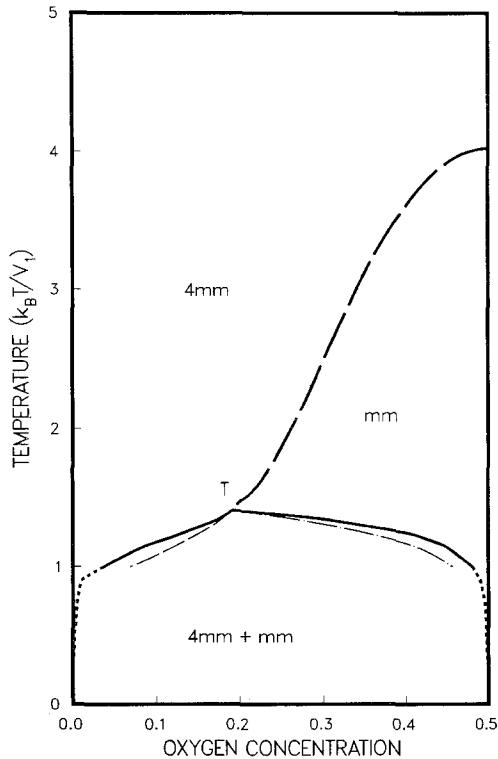


Fig. 2. The CVM phase diagram calculated for $V_1 > 0$, $V_2 = V_3 = -\frac{1}{2}V_1$. Concentration (c_O) is that of the basal plane such that $z = 2c_O + 6$. Second-order transitions are indicated by dashed lines, miscibility gap (phase separation) by full lines. Tricritical point is at point marked T . Thin dashed line is metastable extension of line of second-order transitions, the dot-dash curve is the line of marginal instability for phase separation on the partially filled oxygen sublattice. Tetragonal and orthorhombic phase regions are designated by symbols $4mm$ and mm , respectively.

filled sublattice in the ordered phase. The two-phase region ($4mm + mm$) rapidly spreads out as the temperature is lowered, so that, at absolute zero, the solubility of \circ in the disordered phase and \square in the ordered are nil.

These tangency rules and spinodals are mean-field features and are therefore not strictly valid from an equilibrium statistical mechanical standpoint. In practice, however, the spinodal concept is a very useful one as it provides simple interpretations of phenomena observed under the constraint of slow kinetics at low temperatures. In two dimensions, tricritical points are expected to have nonclassical exponents,⁽²¹⁾ however, so that, in fact, the two-phase coexistence curve at t should be very flat, as calculated by renormalization group methods,^(14,15) and not pointed, as shown in Fig. 2.

The CVM is particularly well suited to the determination of long- and short-range order calculated by means of point, pair, multisite correlation functions. In the present case, 25 independent cluster correlation functions can be evaluated as a function of concentration and temperature. Here we consider only point and second-neighbor pair correlations. Point correlations give directly the fractional site occupancies x_{O}^{α} , x_{O}^{β} , i.e., the probability that a site on the oxygen-rich (α) and oxygen-poor (β) simple square lattices is occupied by an oxygen atom. The appropriate second-neighbor pair correlations give the probability x_2^{α} of finding an O-O pair (actually an O-Cu-O triplet) on the α sublattice. Thus, x_{O} is a measure of long-range order, x_2 of short-range order.

Figure 3 shows the variation with temperature of x_{O}^{α} and x_{O}^{β} for fixed overall concentration $c_{\text{O}} = 0.25$. Under the usual assumption that oxygen vacancies are found exclusively in the basal plane, the planar concentration c_{O} is related to the overall oxygen stoichiometry z by the relation $z = 6 + 2c_{\text{O}}$. A first bifurcation occurs at the second-order transition (around reduced temperature 1.83). Additional bifurcations occur (around 1.38) at the first-order transition. Below that temperature, the oxygen-rich sublattice (α) "phase separates" so that, at equilibrium, the x_{O} plots must follow the heavy lines in Fig. 3, indicating site occupancy of the α and β sublattices in the ordered (mm) phase. Metastable extensions of these lines meet at the tricritical point. The heavy, dashed line represents site occupancy in the disordered phase ($4mm$) in equilibrium with the ordered phase.

The diagram of Fig. 3 is rather more complicated than those obtained by Jorgensen *et al.*⁽¹⁾ from neutron diffraction experiments on $\text{YBa}_2\text{Cu}_3\text{O}_z$. The first-order transition predicted from the present model may occur at a temperature too low to be observed experimentally, however. Hence, the metastable extensions of the first bifurcation (fine lines) may be more relevant to the experimental findings. Furthermore, the experiments were

carried out at constant oxygen partial pressure, not constant oxygen concentration, as was the case for the calculated site occupancies.

The essential role played by O-Cu-O chains along the orthorhombic b axis of $\text{YBa}_2\text{Cu}_3\text{O}_z$ has been mentioned abundantly in the recent literature on superconductivity. It is therefore of interest to determine what the present model can predict concerning short-range pair correlations along these chains. For that purpose, we plot in Fig. 4 the fractional second-neighbor pair occupancy, or pair probability x_2^z in the oxygen-rich sublattice, as a function of temperature, for two fixed average oxygen concentrations $c_{\text{O}} = 0.5$ and 0.33 . It is seen that x_2^z increases as temperature decreases, as expected, until the ordering critical temperature $T_0(c_{\text{O}})$ is reached. The pair concentration then rises rapidly, with sharp change of slope, but then exhibits a marked inflection located in the vicinity of the tricritical temperature. That dx_{O}^z/dT goes through a minimum is undoub-

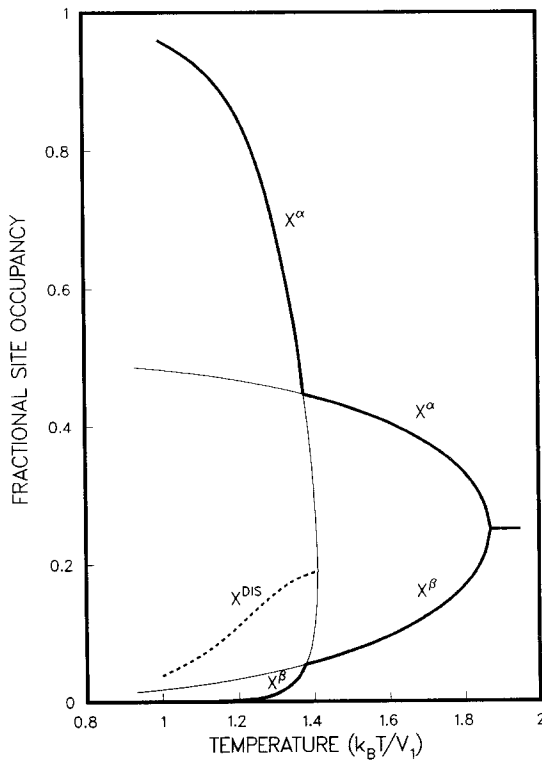


Fig. 3. Oxygen site occupation as function of reduced temperature for fixed average concentration $c_{\text{O}} = 0.25$. Thin lines are metastable extensions. Dashed curve gives site occupancy in the disordered phase in equilibrium with the ordered one.

tedly due to the fact that the α sublattice itself can be regarded as an "open system" whose concentration x_{O}^{α} is steadily increasing while oxygen pair rearrangement is proceeding independently. Both processes contribute to the increase of x_{O}^{α} , but at different rates. Note, that, in Fig. 4, the probabilities x_2^{α} below the first-order phase separation temperature are those of the ordered phase metastable extension.

It is tempting to speculate that such nonmonotonic variation of the slope of the x_2^{α} versus T curves is related to the steplike behavior of the superconducting transition temperature as a function of overall oxygen content, as reported by Cava *et al.*⁽²²⁾ These authors indeed attribute their intriguing results to long- or short-range ordering of oxygen vacancies, although more complicated ordering processes than the simple ones investigated here may be occurring in practice. This matter is currently being studied.

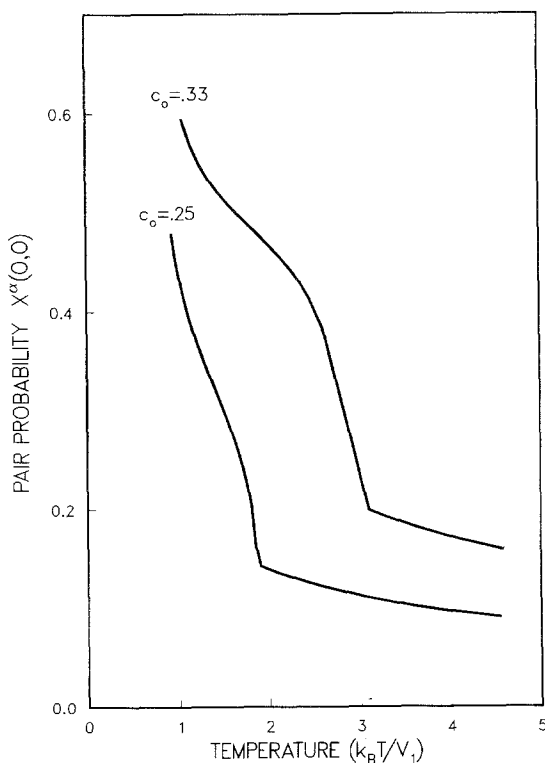


Fig. 4. Second-neighbor oxygen-oxygen pair probabilities as a function of reduced temperature for the two indicated oxygen concentrations. Sharp discontinuities in slope occur at second-order transition.

Finally, let us consider the observation that the tetragonal to orthorhombic transition appears to occur at oxygen content $z \approx 6.5$ regardless of the equilibrium oxygen partial pressure.⁽¹⁾ It may therefore be concluded that the second-order transition line is very steep in the temperature range of interest. This is seen to be the case in the phase diagram of Fig. 1, where, in fact, the transition line has its steepest slope at about $c_O = 0.3$, which comes out to $z = 6.6$ for the overall oxygen, in agreement with experimental findings. The line of second-order transitions is even steeper in the Monte Carlo⁽¹⁶⁾ and renormalization group⁽¹⁵⁾ phase diagrams: there the transition line is almost vertical just above the tricritical point and is located near $c_O = 0.31$ ($z \approx 6.62$), this value being largely insensitive to the ratio V_2/V_1 with $V_1 > 0$, $V_2 < 0$.

In conclusion, it appears that the present model can describe, at least qualitatively, some of the important thermodynamic features of the compound $\text{YBa}_2\text{Cu}_3\text{O}_z$. Better agreement is expected for more realistic models featuring other choices of values for V_1 , V_2 , and V_3 .

ACKNOWLEDGMENTS

The authors are indebted to Dr. J. Kulik for pointing out the need to include both four- and five-point clusters in the CVM and to Marcel Sluiter for the use of his CVM codes as well as for many discussions. Helpful conversations with Drs. H. Zandbergen, F. Herman, and J. Wheeler are also gratefully acknowledged. This work was supported by the Director, Office of Energy Research, Materials Sciences Division, U.S. Department of Energy under contract DE-AC03-76SF00098 and by a National Science Foundation Graduate Fellowship.

REFERENCES

1. J. D. Jorgensen, M. A. Beno, D. G. Hinks, L. Soderholm, K. J. Volin, R. L. Hitterman, J. D. Grace, I. K. Schuller, C. V. Segre, K. Zhang and M. S. Kleefisch, *Phys. Rev. B* **36**: 3608 (1987).
2. D. de Fontaine, L. T. Wille, and S. C. Moss, *Phys. Rev. B* **36**:5709 (1987).
3. L. T. Wille and D. de Fontaine, *Phys. Rev. B* **37**:2227 (1988).
4. G. Van Tendeloo, H. W. Zandbergen, and S. Amelinckx, *Solid State Commun.* **63**:603 (1987).
5. R. Kikuchi, *Phys. Rev.* **81**:988 (1951).
6. H. Bakker, D. O. Welch, and O. W. Lazareth, *Solid State Commun.* **64**:237 (1987).
7. E. Salomons, N. Koeman, R. Brouwer, D. G. de Groot, and R. Griessen, *Solid State Commun.* **64**:1141 (1987).
8. A. Finel and D. de Fontaine, *J. Stat. Phys.* **43**:645 (1987).
9. A. Finel, Thèse de Doctorat, Université Pierre et Marie Curie (1987).
10. J. M. Bell, *Phys. Rev. B* **37**:541 (1988).

11. J. Kulik, private communication.
12. R. Kikuchi, private communication.
13. J. Oitmaa, *J. Phys. A: Math. Gen.* **14**:1159 (1981).
14. P. A. Rikvold, W. Kinzel, J. D. Gunton, and K. Kaski, *Phys. Rev. B* **28**:2686 (1983).
15. F. Claro and V. Kumar, *Surf. Sci.* **119**:L371 (1982).
16. K. Binder and D. P. Landau, *Phys. Rev. B* **21**:1941 (1980).
17. P. A. Slotte, *J. Phys. C: Solid State Phys.* **16**:2935 (1983).
18. D. A. Huse, *Phys. Rev. Lett.* **39**:1121 (1982).
19. S. M. Allen and J. W. Cahn, in *Alloy Phase Diagrams*, L. M. Bennett, T. B. Massalski, and B. C. Griessen, eds., (Materials Research Society Proceedings, 1983), Vol. 19, p. 195.
20. D. de Fontaine, *Solid State Phys.* **34**:73 (1979).
21. J. C. Wheeler, private communication.
22. R. J. Cava, B. Batlogg, C. H. Chen, E. A. Rietman, S. M. Zakuriah, and D. Werder, *Phys. Rev. B* **36**:5719 (1987).